Analyst

PAPER

View Article Online
View Journal | View Issue

Cite this: *Analyst*, 2019, **144**, 4687

An *in cellulo*-activated multicolor cell labeling approach used to image dying cell clearance†

Yilong Shi,[a] Rui Zhu,[b] Zhongwei Xue,[b] Jiahuai Han[a] and Shoufa Han *[b]

Received 17th May 2019,
Accepted 11th June 2019

DOI: 10.1039/c9an00904c

rsc.li/analyst

Dying cell clearance is critical for myriad biological processes such as tissue homeostasis. We herein report an enzyme-activated fluorescence cell labeling approach and its use for multicolor imaging of dying cell clearance. Diacetylated 4-hydroxymandelic acid (DHA)-conjugated dyes give rise to reactive quinone methides upon deacetylation in live cells, which in turn covalently labels cellular proteins. With partner cells tagged with distinct fluorescence, apoptotic cell clearance by Raw 264.7 macrophages and epithelial HeLa cells was captured by confocal microscopy, showing the potential of DHA-based cell labeling for investigating cell–cell interactions.

Approaches to tag cells with distinct fluorescence are valuable tools for cell biology, as evidenced by the use of fluorescent proteins.[1] Alternative to genetically introduced fluorescent proteins, synthetic optical probes are advantageous in several aspects such as tunable fluorescence and ease of functionalization.[2] Because small molecule probes are often susceptible to diffusion or leakage from targeted cells, extensive efforts have been directed at devising imaging agents trappable in cells.[3] Commercial cell-trackers with a reactive succinimidyl ester or chloromethyl moiety allow covalent labeling of cellular proteins *via* amidation or alkylation.[4] This covalent linking improves fluorescence retention in cells and facilitates long-term cell tracking *in vitro* and *in vivo*.[5] Although widely used, different cell-trackers exhibit variations in chemical stability, reactivity or labeling efficiency.[6] Hence, high performance cell labeling, amenable to diverse fluorophores *via* identical chemistry, is desirable in cell imaging.

Cell death routinely occurs in tissue development and homeostasis. Prompt clearance of dying cells is critical for tissue functions while defects in this process have been linked to myriad diseases.[7] Apoptotic cells have been reported to be engulfed by professional phagocytes and non-professional phagocytes such as epithelial cells.[7b,8] Given the engagement of cell death in diverse diseases,[8a,9] approaches to discern the capability of different cell types in dying cell clearance would be of significant biomedical significance. Activity-based probes that could form covalent linkages with enzymes have been widely used in proteomics studies.[10] Quinone methides have been often employed to target hydrolases.[11] Based on these achievements, we applied quinone methide chemistry for fluorescence cell labeling using diacetylated 4-hydroxymandelate (DHA) as the latent protein labeling warhead. Upon deacetylation inside cells, DHA-conjugated dyes self-immolate to yield highly reactive quinone methide–dye dyads, which effectively label intracellular proteins with cognate dyes (Scheme 1) and thus provide distinct fluorescence windows for multicolor imaging of cell–cell interactions.

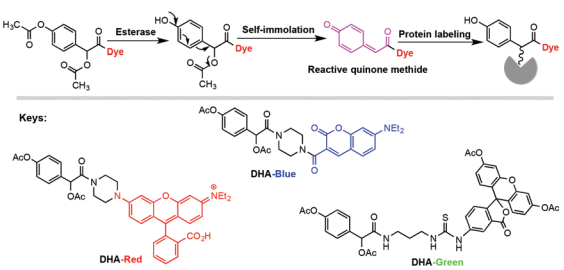

Scheme 1 Fluorescence cell labeling with DHA–dye dyads activatable for cellular deacetylation. In viable cells, DHA undergoes tandem deacetylation and self-immolation to give the reactive quinone methide, which labels cellular proteins with cognate fluorophores. The keys show the chemical structures of DHA-Blue, DHA-Green and DHA-Red, which correspondingly label cells with coumarin of blue fluorescence, fluorescein of green fluorescence and rhodamine of red fluorescence.

[a]*State key Laboratory of Cellular Stress Biology, Innovation Center for Cell Signalling Network, School of Life Sciences, Xiamen University, Xiamen, Fujian, China*
[b]*State Key Laboratory for Physical Chemistry of Solid Surfaces, Department of Chemical Biology, College of Chemistry and Chemical Engineering, the Key Laboratory for Chemical Biology of Fujian Province, The MOE Key Laboratory of Spectrochemical Analysis & Instrumentation, Xiamen University, Xiamen, 361005, China. E-mail: shoufa@xmu.edu.cn; Tel: +86 -0592-2181728*

† Electronic supplementary information (ESI) available: Synthesis and analysis of DHA probes, cell labeling with DHA probes, cytotoxicity of DHA probes, cell staining using DHA-Green and CFSE, dying cell clearance by HeLa cells. See DOI: 10.1039/c9an00904c

Results and discussion

Halogens and carbamates have been previously employed as leaving groups to generate quinone methides (Scheme 2A).[12] We envisioned that optical probes containing diacetylated 4-hydroxymandelate (DHA) could offer a simplified cell labeling approach if the dual acetyl groups might serve respectively as the enzyme-activated group and the leaving group to assist quinone methide formation (Scheme 2B). The advantage of the use of the acetyl moiety over the prior carbamate or halogen as the leaving group is that both the esterase-recognizing moiety and the leaving group, to promote quinone formation, could be installed *via* a simple-step acetylation of 4-hydroxymandate in high yields. As a proof-of-concept, we examined the response of azide-appended DHA (compound **1**) towards sodium methoxide. Removal of the *O*-acetyl group at C-2 prior to that at the C-4 benzene ring would yield compound **2**, whereas the sequentially reversed deacetylation would give rise to a quinone methide which could be quenched by methoxide ions to give compound **3** (Scheme 2C). As expected, two major products of distinct R_f values were identified by TLC analysis (Scheme S1, ESI†). HRMS and H-NMR analyses of the isolated products confirmed the proposed identification of compounds **2** and **3** (Fig. S1–S5, ESI†), validating the applicability of the acetyl group as an effective leaving group to allow quinone methide formation from acetylated DHA.

Given the prevalence of enzymatic deacetylation in mammalian cells,[13] we envisioned that DHA would be an effective platform for deacetylation-triggered covalent cell labeling. In contrast to indiscriminate regio-selectivity of sodium methoxide towards diacetyl groups of DHA (Scheme 2C), enzymes preferentially hydrolyze the *O*-acetyl group at the benzene ring over the C-2 acetyl group due to the steric effects of the bulky dye in the vicinity (C-1), which is beneficial for quinone methide formation and cell labeling. Hence DHA was coupled with rhodamine, coumarin or fluorescein to give DHA-Red, DHA-Blue and DHA-Green (Scheme S1, ESI†) in order to label cells with red, blue, or green fluorescence. Analysis showed that DHA-Red exhibited similar fluorescence to rhodamine under physiological pH conditions (Scheme 2B), indicating that DHA has minimal interference on the fluorescence properties of the incorporated dye. With these compounds, we first assessed the enzymatic activation of DHA *in vitro*. DHA-Red was incubated with esterase from porcine liver or control protein (bovine serum albumin, BSA) and then subjected to SDS-PAGE, respectively. Analysis of the gel revealed esterase-associated rhodamine fluorescence whereas no BSA-associated fluorescence could be observed (Fig. S6, ESI†), showing covalent labeling of esterase with DHA-Red. The selective labeling of esterase over BSA by DHA-Red is consistent with deacetylation-triggered quinone methide formation from DHA-Red (Scheme 2B).

Next, we applied DHA for live cell labeling. HeLa cells were cultured with DHA-Red or AP-Red (rhodamine-conjugated 4-acetoxyphenylacetate) in the presence of Lyso-Tracker Blue specific for lysosomes. AP-Red, differing from DHA-Red in the lack of a C-2 acetyl moiety (Fig. 1A), is incapable of generating the quinone methide upon deacetylation. Compared with the bright rhodamine fluorescence widespread in DHA-Red$^+$ cells, no fluorescence could be identified in cells treated with AP-Red (Fig. 1B), clearly showing that AP-Red is inefficient in staining live cells owing to its incapability to be retained inside cells. The distinct cell labeling with DHA-Red over AP-Red shows the essential role of the DHA moiety for effective cell labeling. To verify covalent protein labeling, DHA-Red$^+$ cells were analyzed by SDS-page. Gel fluorescence analysis revealed that red fluorescence was associated with a plethora of cellular proteins whereas no protein-labeling could be observed in AP-Red treated cells (Fig. 1C, Fig. S7, ESI†), showing that the *in situ* formed quinone methide could diffuse a certain distance and then be captured by surrounding proteins. In addition, DHA-Red effectively labeled diverse cell lines including 3T3, A549, B16F10, Huh-7, U2OS and Raw 264.7 cells (Fig. 2). We also showed that DHA-Red labeled cells in a dose- and incubation time-dependent manner (Fig. S8, ESI†). Finally, it was shown that cell labeling was also effective with DHA-Blue and DHA-Green (Fig. S9 and S10, ESI†). Taken together, these results validate the use of DHA for covalent cell labeling with distinct fluorescence.

After confirming the low cytotoxicity of DHA probes by MTT assay (Fig. S11, ESI†), we compared DHA probes with the commercial cell-tracker (CFSE) for practical cell labeling. HeLa cells were cultivated with 6-carboxyfluorescein diacetate succinimidyl ester (CFSE) or DHA-Green under identical conditions. Flow cytometric analysis showed that DHA-Green$^+$ cells exhibited 7-fold greater fluorescein fluorescence than CFSE$^+$ cells (Fig. S12, ESI†). Next, a time course study was performed to monitor fluorescence retention in DHA- or CFSE-treated cells

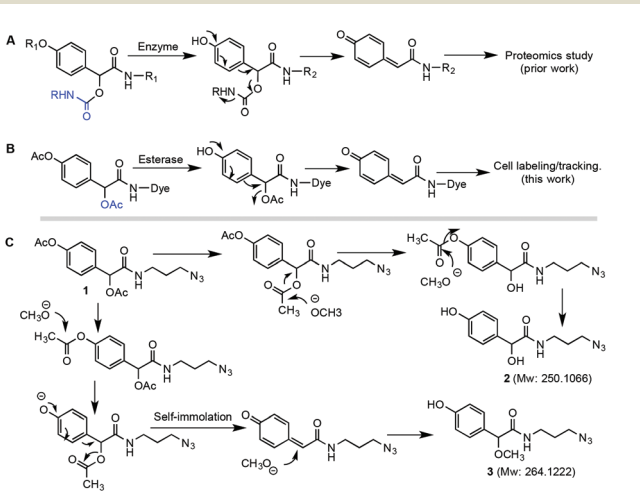

Scheme 2 DHA-based quinone methide formation upon deacetylation. (A) Prior use of carbamates as the leaving group in enzyme-elicited formation of the quinone methide.[12e,f] (B) The use of an acetyl group as the leaving group to allow quinone methide genesis in this work. (C) Proposed mechanisms of the formation of compounds **2** and **3** from region-distinct deacetylation of DHA by methoxide ions.

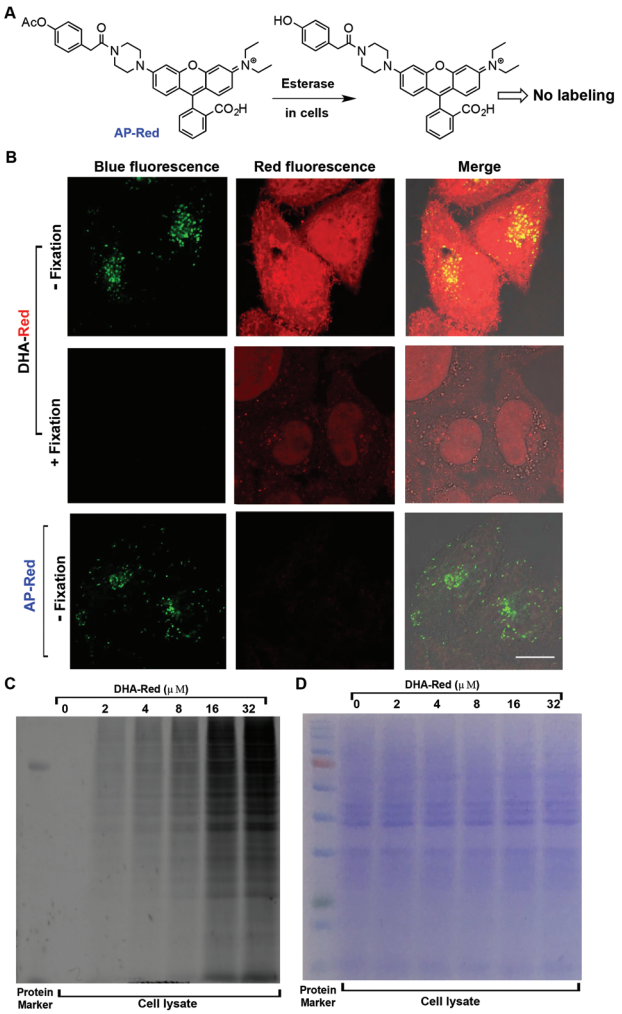

Fig. 1 Covalent cell labeling with DHA-Red. (A) Chemical schematic for the incapability of AP-Red to label cells upon deacetylation. (B) Differential cell labeling with DHA-Red over AP-Red. HeLa cells were incubated with DHA-Red (4 μM) or AP-Red (4 μM) for 1 h in medium containing Lyso-Tracker Blue (4 μM) and then analysed by confocal microscopy. DHA-Red$^+$/Lyso-Tracker Blue$^+$ cells were further fixed with paraformaldehyde, rinsed with fresh medium and then imaged for intracellular fluorescence of rhodamine and Lyso-Tracker Blue. Scale bar: 10 μm. (C/D) Dose-dependent covalent labeling of intracellular proteins with DHA-Red. HeLa cells were cultivated with various levels of DHA-Red (0–32 μM, as indicated) for 1 h and then lysed. Cell lysate was resolved by SDS-page and the gel was detected for rhodamine fluorescence (C) or stained with coomassie blue for total cellular proteins (D).

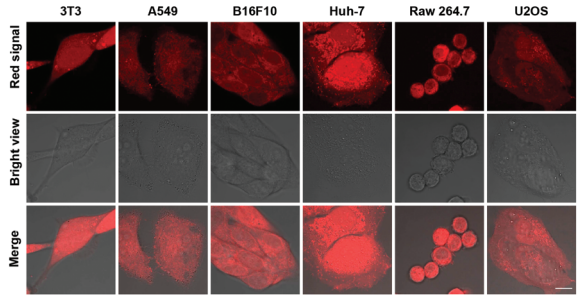

Fig. 2 Effective fluorescence labeling of diverse cell lines with DHA-Red. 3T3, A549, B16F10, Huh-7, Raw 264.7 macrophages and U2OS cells were cultivated with DHA-Red (4 μM) in DMEM for 1 h and then examined for intracellular rhodamine fluorescence by confocal microscopy. Scale bar: 10 μm.

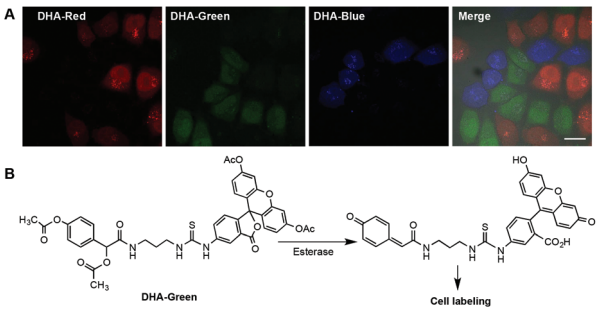

Fig. 3 The use of DHA for fluorescence tracking of multiplexed cells. (A) Confocal fluorescence microscopy images of multiplexed DHA-labeled cells. HeLa cells pretreated with DHA-Blue, DHA-Green or DHA-Red were mixed, cocultured in fresh cell culture medium for 24 h, and then imaged by confocal microscopy. Scale bar: 20 μm. (B) Chemistry of cell-mediated activation of DHA-Green, which undergoes deacetylation triggered formation of a fluorescein fluorophore/self-immolation to give the quinone methide for fluorescence cell labeling.

over cell proliferation. DHA-associated red, blue and green signals, detectable in cells after 48 h cell growth, decreased over time in patterns similar to those of CFSE (Fig. S12, ESI†). We finally examined the capability of DHA probes for cell multiplexing. Three cell populations, independently pre-stained with DHA-Blue, DHA-Red, or DHA-Green, were mixed and then co-cultured for 24 h. Confocal microscopy imaging showed cell specific blue, green, or red fluorescence, while no detectable fluorescence cross contamination (Fig. 3). Collectively, these findings validate the applicability of DHA probes for cell tracking in multiplexed settings.

Cell death routinely occurs in myriad patho-physiological processes. Prompt clearance of dying cells is critical for tissue health such as tissue repair and resolution of inflammation.[7] To image dying cell clearance, we first determined the capability of DHA probes to track dying cells. HeLa cells expressing receptor-interacting protein 3 (RIP3$^+$) were labeled with DHA-Red, DHA-Blue or DHA-Green, and then treated for 0–12 h with Smac/human Tumor Necrosis Factor-a (TNF) to trigger apoptosis, or with Smac/TNF/Z-VAD to trigger necrosis.[14] Bright fluorescence was identified in apoptotic cells or cell bodies formed upon necrosis in the whole cell death course (Fig. S13, ESI†), showing the use of DHA probes to track dying cells. We then applied DHA-probes to image the clearance of dead cells. Raw 264.7 macrophages pre-labeled with DHA-Red were cultivated with Smac/TNF to induce apoptosis. The resultant DHA-Red$^+$ apoptotic macrophages were then co-cultured for 6 h with DHA-Blue$^+$ viable Raw 264.7 cells. Confocal microscopy analysis clearly revealed the wide pres-

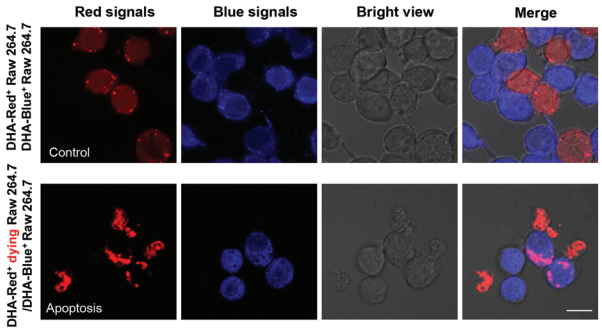

Fig. 4 Engulfment of apoptotic Raw 264.7 macrophages by viable Raw 264.7 cells. Raw 264.7 macrophages were stained with DHA-Red and then treated with Smac/TNF to induce apoptosis. The DHA-Red$^+$ apoptotic cells or viable DHA-Red$^+$ Raw 264.7 cells (control) were further co-cultured for 6 h with DHA-Blue$^+$ Raw 264.7 cells before confocal microscopic analysis. Scale bar: 10 μm.

ence of red fluorescence patches in DHA-Blue$^+$ viable cells. In contrast, no red signals could be observed in DHA-Blue$^+$ viable Raw 264.7 cells co-cultured with DHA-Red$^+$ viable Raw 264.7 cells (Fig. 4), showing effective phagocytosis of apoptosed cells by Raw 264.7 macrophages.

Besides phagocytes (macrophages), certain non-professional phagocytes have been reported to be capable of removing apoptotic cells.[15] For instance, bronchial epithelial cells engulf apoptotic cells and influence airway inflammation.[8a,16] To discern the capability of somatic cells in engulfing dying cells, HeLa cells, a human cervical carcinoma epithelial cell line, were labeled with DHA-Blue and then challenged with apoptotic DHA-Red$^+$ Raw 264.7 cells. Red-emissive cell bodies were identified to locate sporadically in DHA-Blue$^+$ HeLa cells (Fig. 5), showing the capability of HeLa cells to engulf apoptotic cells. Finally, the uptake of apoptotic HeLa cells by HeLa cells was examined with the aid of DHA labeling. As shown in Fig. 6, viable HeLa cells are capable of taking up apoptotic HeLa cells. Collectively these results validate the utility of DHA-conferred cell labeling to image dying cell clearance by distinct host cells.

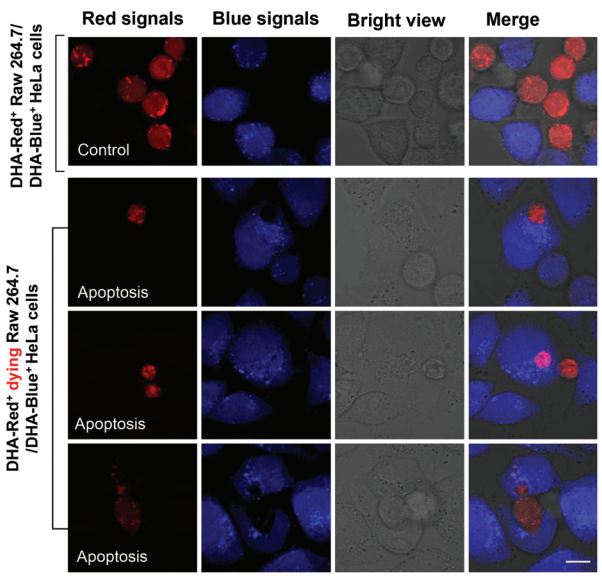

Fig. 5 Engulfment of apoptotic Raw 264.7 macrophages by viable HeLa cells. DHA-Blue$^+$ viable HeLa cells were co-cultured for 6 h with DHA-Red$^+$ apoptotic Raw 264.7 cells or viable DHA-Red$^+$ Raw 264.7 cells (control), and then probed by confocal microscopy. On dying cell clearance, three independent images were included to show the contact or engulfment of apoptotic cells per cell body with viable HeLa cells. Scale bar: 10 μm.

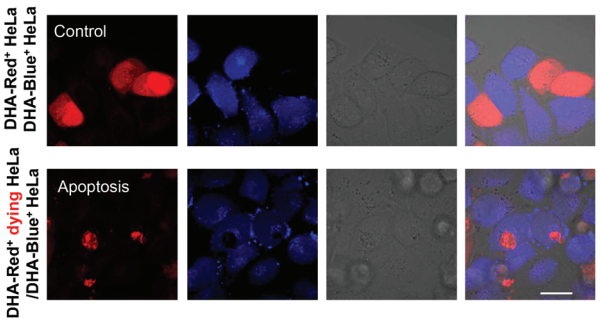

Fig. 6 Engulfment of apoptotic HeLa cells by HeLa cells. DHA-Blue$^+$ HeLa cells were cocultured for 6 h with apoptotic DHA-Red$^+$ HeLa cells or viable DHA-Red$^+$ HeLa cells (control), and then visualized by confocal microscopy. Scale bar: 20 μm.

Conclusions

Long-term fluorescence tagging of cells is of use to investigate cell–cell interactions linked to diverse biological events and diseases. We have shown the use of diacetylated 4-hydroxymandelate (DHA), a latent protein-labeling warhead activatable in viable cells, for high performance fluorescence cell labeling. Stably trapped in dying cells and multiplexed cells, DHA-based cell labeling enables visualization and differentiation of dying cell clearance by macrophages, and HeLa epithelial cells. We envision that DHA technology could be readily extended to tag cells with near infrared fluorophores or magnetic resonance imaging reagents, which would be beneficial for *in vivo* imaging or tracking of cell–cell interactions.

Experimental procedure

Materials and methods

LysoTrackers and Cell-Tracker CFSE were obtained from Thermo Fisher. Other dyes were purchased from Bioluminor, Xiamen. All other chemicals were purchased from Sigma unless specified. The cell lines were obtained from the American Type Culture Collection (ATCC). All of the cell lines used in this work are obtained from ATCC, USA. All cells were maintained in Dulbecco's modified Eagle's medium (DMEM), supplemented with 10% fetal bovine serum, 2 mM L-glutamine, 100 IU penicillin, and 100 mg mL^{-1} streptomycin

at 37 °C in a humidified incubator under 5% CO_2, with the exception that 1% nonessential amino acids were added to the aforementioned culture for Raw 264.7 cell culturing.

The fluorescence spectra were recorded on a SpectraMax M5. Confocal fluorescence microscopic imaging was performed on a Zeiss LSM 780 using the following filters: λ_{ex} = 405 nm/λ_{em} = 420–460 nm for DHA-Blue and MitoTracker blue, λ_{ex} = 488 nm/λ_{em} = 499–553 nm for CFSE and DHA-Green, λ_{ex} = 561 nm/λ_{em} = 585–733 nm for DHA-Red and Lyso-Tracker Red. The fluorescence of rhodamine in cells was shown in red in the figures while that of CFSE and DHA-Green was shown in green. Images of merged fluorescence were processed using Photoshop CC2014. Quantitative imaging analysis was carried out on unprocessed images using ImageJ software. A graph was generated using GraphPad Prism7 and Origin 8.0 software. Flow cytometry was performed on a BD Fortessa, the fluorescence emission of rhodamine was recorded with an FL2 filter (590–630 nm) using a λ_{ex} of 561 nm, and the fluorescence emission of coumarin was recorded with the FL2 filter (590–630 nm) using the λ_{ex} of 561 nm. 10 000 cells were gated under identical conditions and analyzed. The data were processed using GraphPad Prism7.

Synthesis of compound 1 (Scheme S1 ESI†). 4-Hydroxymandelic acid (4 g, 21.5 mmol) and triethylamine (TEA, 8.7 g, 86.0 mmol) were dissolved in CH_2Cl_2 (200 mL). To the solution was added acetyl chloride (5.1 g, 64.5 mmol). The mixture was stirred for 0.5 h, and then washed with an aqueous solution of saturated sodium bicarbonate (80 mL). The organic phase was washed with water (100 mL), and then concentrated under reduced pressure to yield diacetylated 4-hydroxymandelic acid (DHA, 4.5 g, 83%), which was used without further purification. DHA (2 g, 7.93 mmol) and 3-azidopropyl-1-amine (0.72 g, 9.52 mmol) were dissolved in CH_2Cl_2 (50 mL) containing 1-(3-dimethylaminopropyl)-3-ethylcarbodiimide hydrochloride (EDC, 2.28 g, 11.91 mmol) and triethylamine (TEA, 2.41 g, 23.85 mmol). The reaction mixture was stirred overnight, and then concentrated. The residue was subjected to silica gel chromatography (petroleum ether/ethyl acetate = 1/3) to yield **1** (2.3 g, 87%). ^{1}H-NMR (500 MHz, DMSO-d_6) δ 8.35 (t, J = 5.8 Hz, 1H), 7.48 (d, J = 8.6 Hz, 2H), 7.14 (d, J = 8.6 Hz, 2H), 5.81 (s, 1H), 3.27 (t, J = 6.8 Hz, 4H), 3.12 (dp, J = 21.8, 6.7 Hz, 2H), 2.27 (s, 3H), 2.12 (s, 3H), 1.63 (p, J = 6.9 Hz, 2H). ^{13}C-NMR (126 MHz, DMSO) δ 170.14, 169.61, 168.39, 151.04, 133.81, 128.96, 122.34, 75.02, 48.65, 36.28, 28.71, 21.28, 21.12. MS (ES+) calc'd for $C_{15}H_{18}N_4NaO_5^+$ (M + Na) m/z 357.12, Found 357.23.

Deacetylation of compound 1 (Scheme S1 ESI†). To a solution of compound **1** (700 mg, 2.1 mmol) in anhydrous MeOH (5.0 mL) was added $NaOCH_3$ (0.5 mmol). The mixture was stirred at room temperature for 3 h, and then analyzed by TLC (petroleum ether/ethyl acetate = 1/2). After the reaction was complete, Amberlys® 15 ion-exchange resin was added to neutralize the solution. The solution was concentrated under reduced pressure and the residue was chromatographed (silica gel, petroleum ether/ethyl acetate = 1/2) to yield compounds **2** (220 mg, 42%) and **3** (300 mg, 54%). Compound **2**: ^{1}H-NMR (500 MHz, DMSO-d_6) δ 9.31 (s, 1H), 8.00 (t, J = 6.0 Hz, 1H), 7.17 (d, J = 8.3 Hz, 2H), 6.69 (d, J = 8.6 Hz, 2H), 5.91 (d, J = 4.4 Hz, 1H), 4.77 (d, J = 4.3 Hz, 1H), 3.29 (t, J = 6.9 Hz, 2H), 3.13 (d, J = 6.4 Hz, 2H), 1.66 (p, J = 6.8 Hz, 2H). ^{13}C-NMR (126 MHz, DMSO) δ 173.15, 157.16, 132.25, 128.23, 115.12, 73.79, 48.90, 36.10, 28.94. MS (ES+) calc'd for $C_{11}H_{14}N_4NaO_3^+$ (M + Na) m/z 273.10, Found 273.13. Compound **3**: ^{1}H NMR (500 MHz, DMSO-d_6) δ 9.42 (s, 1H), 8.09 (t, J = 5.9 Hz, 1H), 7.15 (d, J = 8.5 Hz, 2H), 6.72 (d, J = 8.6 Hz, 2H), 4.46 (s, 1H), 3.29 (t, J = 6.8 Hz, 2H), 3.22 (s, 3H), 3.13 (q, J = 6.6 Hz, 2H), 1.66 (p, J = 6.8 Hz, 2H). ^{13}C-NMR (126 MHz, DMSO) δ 170.32, 157.20, 128.39, 128.35, 114.88, 83.11, 56.39, 48.43, 35.67, 28.44. MS (ES+) calc'd for $C_{12}H_{16}N_4NaO_3^+$ (M + Na) m/z 287.11, Found 287.18.

Synthesis of DHA-Red and AP-Red (Scheme S2, ESI†). To a solution of DHA (1.00 g, 4.0 mmol) or 2-(4-hydroxyphenyl) acetic acid in anhydrous CH_2Cl_2 (15 mL) were added TEA (1.21 g, 12.0 mmol), EDC (0.96 g, 5.0 mmol) and amino-containing rhodamine (1.83 g 4.0 mmol) sequentially at room temperature. After stirring for 120 min, the reaction mixture was washed with aqueous HCl (1 M, 20 mL) and then water (20 mL). The organic layers were dried over anhydrous Na_2SO_4, filtered, and then concentrated. The resulting residues were resolved by flash chromatography to give DHA-Red (70%) or AP-Red (80%). **DHA-Red**: ^{1}H-NMR (500 MHz, chloroform-d) δ 7.98 (d, J = 7.5 Hz, 1H), 7.62 (t, J = 7.4 Hz, 1H), 7.57 (t, J = 7.4 Hz, 1H), 7.48 (d, J = 8.6 Hz, 2H), 7.15 (t, J = 8.9 Hz, 3H), 6.63–6.57 (m, 2H), 6.54 (d, J = 8.9 Hz, 1H), 6.48 (dd, J = 8.8, 2.5 Hz, 1H), 6.42 (d, J = 2.5 Hz, 1H), 6.33 (dd, J = 9.0, 2.6 Hz, 1H), 6.28 (s, 1H), 3.81–3.69 (m, 2H), 3.68–3.59 (m, 1H), 3.51–3.41 (m, 1H), 3.33 (q, J = 7.0 Hz, 4H), 3.27–3.09 (m, 3H), 2.89–2.75 (m, 1H), 2.28 (d, J = 1.5 Hz, 3H), 2.16 (s, 3H), 1.15 (t, J = 7.0 Hz, 6H). ^{13}C-NMR (126 MHz, $CDCl_3$) δ 170.50, 169.70, 169.07, 166.40, 153.12, 153.00, 152.77, 152.06, 151.41, 149.53, 134.70, 131.46, 129.55, 129.39, 128.86, 128.84, 127.36, 124.72, 124.03, 122.34, 111.79, 111.75, 110.51, 108.28, 105.35, 102.48, 97.57, 84.63, 72.49, 47.97, 44.97, 44.45, 41.93, 21.12, 20.81, 12.53. MS (ES+) calc'd for $C_{40}H_{40}N_3O_8^+$ (M + H) m/z 690.28, Found 690.28199. **AP-Red:** ^{1}H-NMR (500 MHz, chloroform-d) δ 7.98 (d, J = 7.5 Hz, 1H), 7.63 (t, J = 7.4 Hz, 1H), 7.57 (t, J = 7.4 Hz, 1H), 7.29–7.22 (m, 2H), 7.16 (d, J = 7.6 Hz, 1H), 7.04 (d, J = 8.2 Hz, 2H), 6.66–6.58 (m, 2H), 6.55 (d, J = 8.9 Hz, 1H), 6.50 (dd, J = 8.9, 2.4 Hz, 1H), 6.42 (d, J = 2.5 Hz, 1H), 6.33 (dd, J = 8.9, 2.5 Hz, 1H), 3.80–3.74 (m, 2H), 3.72 (s, 2H), 3.59–3.51 (m, 2H), 3.33 (q, J = 7.0 Hz, 4H), 3.22–3.13 (m, 2H), 3.09–3.00 (m, 2H), 2.27 (s, 3H), 1.15 (t, J = 7.0 Hz, 6H). ^{13}C-NMR (126 MHz, $CDCl_3$) δ 169.72, 169.40, 169.35, 153.07, 153.03, 152.80, 152.19, 149.56, 134.72, 132.44, 129.71, 129.42, 128.87, 128.82, 127.39, 124.74, 124.05, 121.85, 111.77, 110.40, 108.30, 105.36, 102.40, 97.56, 84.79, 77.38, 48.32, 48.08, 45.64, 44.46, 41.39, 40.07, 21.13, 12.54. MS (ES+) calc'd for $C_{38}H_{38}N_3O_6^+$ (M + H) m/z 632.28, Found 632.27552.

Synthesis of DHA-Blue (Scheme S3, ESI†). To a solution of DHA (1.00 g, 4.0 mmol) and TEA (1.21 g, 12.0 mmol) in anhydrous CH_2Cl_2 (15 mL) were added EDC (0.96 g, 5.0 mmol) and piperizine-conjugated coumarin (1.3 g, 4.0 mmol). The solution was stirred at room temperature for 2 h, and then washed

with aqueous HCl (1.0 M, 30 mL) and then water (25 ml). The organic layer was dried over anhydrous Na_2SO_4, filtered, and then concentrated. The residue was subjected to silica gel flash chromatography to give DHA-Blue in 80% yield. ^{1}H NMR (500 MHz, chloroform-*d*) δ 7.85 (s, 1H), 7.46 (s, 2H), 7.29 (d, J = 8.4 Hz, 2H), 7.15 (s, 2H), 6.60 (d, J = 8.9 Hz, 1H), 6.46 (s, 1H), 6.26 (s, 1H), 3.73 (s, 5H), 3.43 (q, J = 7.0 Hz, 7H), 2.30 (s, 3H), 2.17 (s, 3H), 1.22 (t, J = 7.0 Hz, 6H). ^{13}C NMR (125 MHz, $CDCl_3$) δ 170.53, 169.02, 166.53, 159.15, 157.36, 151.89, 151.45, 131.30, 129.99, 129.45, 122.37, 115.37, 109.48, 107.72, 96.90, 77.27, 72.51, 46.96, 44.97, 21.12, 20.78, 12.40. MS (ES+) calc'd for $C_{30}H_{33}N_3NaO_8^+$ (M + Na) m/z 586.22, Found 586.21656.

Synthesis of DHA-Green (Scheme S3, ESI†). Compound **1** (1.00 g 4.0 mmol) was dissolved in 10 mL MeOH containing 10% Pd/C (50 mg). The solution was stirred under hydrogen for 24 h, and then filtered. The filtrate was concentrated under reduced pressure. The residue was dissolved in DMF and added dropwise to a solution of fluorescein isothiocyanate (1.57 g, 4.0 mmol) in DMF (10 mL) containing TEA (0.81 g, 8.0 mmol). The mixture was stirred at room temperature for 30 min. The solution was concentrated under reduced pressure, and the residue was dissolved in 10 ml CH_2Cl_2 containing acetic anhydride (4.08 g, 40.0 mmol) and TEA (0.81 g, 8.0 mmol). The solution was stirred at room temperature for 2 h. After the removal of the solvent, the residue was purified by flash chromatography to give DHA-Green in 50% yield. ^{1}H-NMR (500 MHz, DMSO-d_6) δ 10.02 (s, 1H), 8.40 (t, J = 5.7 Hz, 1H), 8.35 (s, 1H), 8.11–8.01 (m, 1H), 7.82–7.73 (m, 1H), 7.51 (d, J = 8.3 Hz, 2H), 7.36–7.26 (m, 3H), 7.15 (d, J = 8.3 Hz, 2H), 6.95 (q, 4H), 5.85 (s, 1H), 4.03 (q, J = 7.1 Hz, 1H), 3.59–3.44 (m, 2H), 3.24–3.07 (m, 2H), 2.29 (s, 6H), 2.27 (s, 3H), 2.13 (d, J = 2.9 Hz, 3H), 1.99 (s, 2H), 1.71 (p, J = 7.0 Hz, 2H). ^{13}C-NMR (125 MHz, DMSO) δ 170.78, 170.11, 169.62, 169.29, 168.69, 168.52, 152.49, 151.29, 151.05, 133.88, 129.54, 129.01, 122.37, 119.05, 116.77, 110.93, 81.38, 75.02, 60.21, 36.67, 29.08, 21.30, 21.27, 21.21, 21.16, 14.54. MS (ES+) calc'd for $C_{40}H_{35}N_3O_{12}S^+$ (M + Na) m/z 804.18, Found 804.18614.

Enzymatic activation of DHA-Red *in vitro*. Esterase from porcine liver (1.5 μg, Sigma) or bovine serum albumin (BSA, 1.5 μg, Sigma) was incubated with DHA-Red (0, 200, and 400 μM) in water containing 20% DMSO. The solutions were maintained at 37 °C for 1 h, and then diluted with 2 × SDS sample buffer. The resulting solutions were resolved using SDS PAGE gel. The gels were imaged for protein associated fluorescence and then stained with coomassie blue to detect total proteins.

Comparison of cell labeling with DHA-Red over AP-Red. HeLa cells were incubated with DHA-Red (4 μM) or AP-Red (4 μM) in cell culture medium containing LysoTracker Blue (1 μM) for 1 h and then analyzed by confocal fluorescence microscopy. The cells were then analyzed by confocal fluorescence microscopy for signals of DHA-Red and LysoTracker Blue.

SDS-PAGE analysis of cells treated with DHA-Red or AP-Red. HeLa cells were stained with DHA-Red (4 μM) or AP-Red (4 μM) in cell culture medium for 1 h and then washed with PBS three times. The cells were lysed and the lysates were resolved by SDS-page. The gels were imaged for protein associated fluorescence and then stained with coomassie blue to detect total proteins.

Cytotoxicity of dye-labeled DHA. HeLa cells were cultured in 48-well cell culture plates with cell culture medium containing DHA-Red, DHA-Blue, or DHA-Green (0, 2, 4, and 8 μM for 0 h, 24 h or 48 h). The cell number and cell viability were determined by MTT assay.

Comparison of DHA probes with commercial CFSE for cell labeling. HeLa cells were incubated with DHA-Red (4 μM), DHA-Blue (4 μM), DHA-Green (4 μM), or CFSE (4 μM) in serum-free DMEM for 1 h, and then analyzed by confocal fluorescence microscopy. The aforementioned cells were further incubated in serum-free DMEM for 0, 24, or 48 h, and then analyzed by flow cytometry for intracellular fluorescence.

Labeling of different cell lines with DHA-Red. B16F10, A549, 293T, CHO, L929, and Raw 264.7 macrophages were incubated in DMEM supplemented with DHA-Red (4 μM) for 1 h. The cells were washed with DMEM and then analyzed by confocal fluorescence microscopy.

Multiplexing of cells labeled with different DHA probes. HeLa cells were cultured in DMEM containing DHA-Red (4 μM), DHA-Blue (4 μM), or DHA-Green (4 μM) for 1 h. The three cell populations were rinsed with fresh DMEM, mixed, co-cultured in fresh DMEM for 24 h, and then visualized by confocal fluorescence microscopy.

Retention of DHA-conferred fluorescence in cells undergoing apoptosis or necrosis. For necroptosis: RIP3$^+$ HeLa cells were cultured in DMEM spiked with DHA-Red (4 μM), DHA-Blue (4 μM), or DHA-Green (4 μM) for 1 h, and then washed with fresh DMEM 3 times. The cells were rested in DMEM for 10 min, and then further cultivated for 0–12 h in DMEM containing human tumor necrosis factor-a (h-TNF, 120 ng mL^{-1})/Smac mimetic (Smac, 400 nM) to trigger necrosis. The cells were harvested for flow cytometric analysis. For apoptosis: RIP3$^+$ HeLa cells were cultured in DMEM spiked with DHA-Red (4 μM), DHA-Blue (4 μM), or DHA-Green (4 μM) for 1 h, and then washed with DMEM 3 times. The cells were rested in DMEM for 20 min, and then cultivated in DMEM containing h-TNF (60 ng mL^{-1})/Smac (400 nM/Z-VAD (40 μM) for 12 h to trigger apoptosis before flow cytometric analysis.

Imaging engulfment of apoptotic Raw 264.7 cells by Raw 264.7 cells. Raw 264.7 cells were cultured in DMEM spiked with DHA-Blue (4 μM) for 1 h, and then washed with DMEM 3 times. The cells were rested in DMEM for 20 min, and then further cultivated in DMEM containing TNF (120 ng mL^{-1})/Smac (400 nM) for 24 h to trigger apoptosis. In parallel Raw 264.7 cells were cultured in DMEM spiked with DHA-Red (4 μM) for 1 h, and then washed 3 times. The resultant Raw 264.7 cells were mixed and cocultured with DHA-Blue-treated apoptotic DHA-Blue$^+$ Raw 264.7 cells in DMEM for 6 h before confocal fluorescence microscopy analysis.

Imaging engulfment of apoptotic Raw 264.7 cells by HeLa cells. Raw 264.7 cells were cultured in DMEM spiked with DHA-Red (4 μM) for 1 h. The cells were washed with fresh

DMEM 3 times, rested in DMEM for 20 min, and then cultivated in DMEM contained TNF (120 ng mL^{-1})/Smac (400 nM) for 24 h to trigger apoptosis. In parallel, HeLa cells were cultured in DMEM spiked with DHA-Blue (4 μM) for 1 h in a 24-well cell culture plate, and then washed 3 times. The resultant HeLa cells were mixed and co-cultured with DHA-Red^+ apoptotic Raw 264.7 cells in DMEM for 6 h and then analyzed by confocal fluorescence microscopy.

Imaging engulfment of apoptotic HeLa cells by HeLa cells. HeLa cells were cultured in DMEM spiked with DHA-Red (4 μM) for 1 h. After washing with fresh DMEM 3 times, the cells were rested in DMEM for 20 min, and then cultured in DMEM containing h-TNF (120 ng mL^{-1})/Smac (400 nM) for 24 h to trigger apoptosis. In parallel HeLa cells were cultured in DMEM spiked with DHA-Blue (4 μM) for 1 h, and then washed 3 times. The resultant DHA-$Blue^+$ HeLa cells were mixed and co-cultured with DHA-$Blue^+$ apoptotic HeLa cells in DMEM for 6 h and then analyzed by confocal fluorescence microscopy.

Conflicts of interest

There are no conflicts to declare.

Acknowledgements

This work was supported by grants from the National Natural Science Foundation of China (81788101, 91854106, 21775130, and 21572189).

Notes and references

1 J. Lippincott-Schwartz and G. H. Patterson, *Science*, 2003, **300**, 87.
2 A. P. de Silva, H. Q. Gunaratne, T. Gunnlaugsson, A. J. Huxley, C. P. McCoy, J. T. Rademacher and T. E. Rice, *Chem. Rev.*, 1997, **97**, 1515.
3 (*a*) T. Jiang, E. S. Olson, Q. T. Nguyen, M. Roy, P. A. Jennings and R. Y. Tsien, *Proc. Natl. Acad. Sci. U. S. A.*, 2004, **101**, 17867; (*b*) A. Razgulin, N. Ma and J. Rao, *Chem. Soc. Rev.*, 2011, **40**, 4186; (*c*) H. Shi, R. T. Kwok, J. Liu, B. Xing, B. Z. Tang and B. Liu, *J. Am. Chem. Soc.*, 2012, **134**, 17972; (*d*) Z. Wang, S. Chen, J. W. Lam, W. Qin, R. T. Kwok, N. Xie, Q. Hu and B. Z. Tang, *J. Am. Chem. Soc.*, 2013, **135**, 8238; (*e*) Z. Xue, E. Zhang, J. Liu, J. Han and S. Han, *Angew. Chem., Int. Ed.*, 2018, **57**, 10096.
4 A. B. Lyons, *Immunol. Cell Biol.*, 1999, **77**, 509.
5 (*a*) V. B. Gibson, R. A. Benson, K. J. Bryson, I. B. McInnes, C. M. Rush, G. Grassia, P. Maffia, E. J. Jenkinson, A. J. White, G. Anderson, J. M. Brewer and P. Garside, *Blood*, 2012, **119**, 2545; (*b*) F. Progatzky, M. J. Dallman and C. Lo Celso, *Interface Focus*, 2013, **3**, 20130001.
6 W. Zhou, H. C. Kang, M. O'Grady, K. M. CHambers, B. Dubbels, P. Melquist and K. R. Gee, *J. Biol. Methods*, 2016, **3**, e36.
7 (*a*) P. M. Henson, *Nat. Immunol.*, 2005, **6**, 1179; (*b*) S. Nagata, R. Hanayama and K. Kawane, *Cell*, 2010, **140**, 619.
8 (*a*) I. J. Juncadella, A. Kadl, A. K. Sharma, Y. M. Shim, A. Hochreiter-Hufford, L. Borish and K. S. Ravichandran, *Nature*, 2013, **493**, 547; (*b*) W. Wood, M. Turmaine, R. Weber, V. Camp, R. A. Maki, S. R. McKercher and P. Martin, *Development*, 2000, **127**, 5245; (*c*) D. J. Baker, T. Wijshake, T. Tchkonia, N. K. LeBrasseur, B. G. Childs, B. van de Sluis, J. L. Kirkland and J. M. van Deursen, *Nature*, 2011, **479**, 232; (*d*) T. Ichimura, E. J. Asseldonk, B. D. Humphreys, L. Gunaratnam, J. S. Duffield and J. V. Bonventre, *J. Clin. Invest.*, 2008, **118**, 1657.
9 C. Z. Han, I. J. Juncadella, J. M. Kinchen, M. W. Buckley, A. L. Klibanov, K. Dryden, S. Onengut-Gumuscu, U. Erdbrugger, S. D. Turner, Y. M. Shim, K. S. Tung and K. S. Ravichandran, *Nature*, 2016, **539**, 570.
10 (*a*) M. J. Evans and B. F. Cravatt, *Chem. Rev.*, 2006, **106**, 3279; (*b*) C. P. Lu, C. T. Ren, S. H. Wu, C. Y. Chu and L. C. Lo, *ChemBioChem*, 2007, **8**, 2187.
11 (*a*) D. H. Kwan, H. M. Chen, K. Ratananikom, S. M. Hancock, Y. Watanabe, P. T. Kongsaeree, A. L. Samuels and S. G. Withers, *Angew. Chem., Int. Ed.*, 2011, **50**, 300; (*b*) L. C. Lo, T. L. Pang, C. H. Kuo, Y. L. Chiang, H. Y. Wang and J. J. Lin, *J. Proteome Res.*, 2002, **1**, 35; (*c*) S. Halazy, V. Berges, A. Ehrhard and C. Danzin, *Bioorg. Chem.*, 1990, **18**, 330; (*d*) C. S. Tsai, Y. K. Li and L. C. Lo, *Org. Lett.*, 2002, **4**, 3607.
12 (*a*) Z. Gao, A. J. Thompson, J. C. Paulson and S. G. Withers, *Angew. Chem., Int. Ed.*, 2018, **57**, 13538; (*b*) K. D. Janda, L. C. Lo, C. H. Lo, M. M. Sim, R. Wang, C. H. Wong and R. A. Lerner, *Science*, 1997, **275**, 945; (*c*) N. W. Polaske, B. D. Kelly, J. Ashworth-Sharpe and C. Bieniarz, *Bioconjugate Chem.*, 2016, **27**, 660; (*d*) Q. Wang, U. Dechert, F. Jirik and S. G. Withers, *Biochem. Biophys. Res. Commun.*, 1994, **200**, 577; (*e*) R. Zhu, S. Wang, Z. Xue, J. Han and S. Han, *Chem. Commun.*, 2018, **54**, 11566; (*f*) T. Komatsu, K. Kikuchi, H. Takakusa, K. Hanaoka, T. Ueno, M. Kamiya, Y. Urano and T. Nagano, *J. Am. Chem. Soc.*, 2006, **128**, 15946.
13 (*a*) H. S. Mellert and S. B. McMahon, *Trends Biochem. Sci.*, 2009, **34**, 571; (*b*) M. Haberland, R. L. Montgomery and E. N. Olson, *Nat. Rev. Genet.*, 2009, **10**, 32; (*c*) S. Pillai, A. Cariappa and S. P. Pirnie, *Trends Immunol.*, 2009, **30**, 488; (*d*) D. Bratosin, L. Mitrofan, C. Palii, J. Estaquier and J. Montreuil, *Cytometry, Part A*, 2005, **66**, 78.
14 S. He, L. Wang, L. Miao, T. Wang, F. Du, L. Zhao and X. Wang, *Cell*, 2009, **137**, 1100.
15 C. D. Gregory and J. D. Pound, *Apoptosis*, 2010, **15**, 1029.
16 H. Jyonouchi, *Apoptosis*, 1999, **4**, 407.